doi:10.1093/brain/awn095 *Brain* (2008), **131**, 1516–1527

Loss of GABAergic neurons in the subiculum and its functional implications in temporal lobe epilepsy

Andreas Knopp,[1,2] Christiane Frahm,[3] Pawel Fidzinski,[1,2] Otto W. Witte[3] and Joachim Behr[1,2]

[1]Department of Psychiatry and Psychotherapy, Charité-Universitätsmedizin Berlin, Charitéplatz 1, 10117, [2]Institute for Neurophysiology, Charité-Universitätsmedizin Berlin, Tucholskystrasse 2, 10117 Berlin and [3]Department of Neurology, Friedrich-Schiller-University, Erlanger Allee 101, 07745 Jena, Germany

Correspondence to: Joachim Behr, Dept. of Psychiatry and Psychotherapy, Charité-Universitätsmedizin Berlin, Charitéplatz 1, 10117 Berlin, Germany
E-mail: joachim.behr@charite.de

Clinical and experimental evidence suggest that the subiculum plays an important role in the maintenance of temporal lobe seizures. Using the pilocarpine-model of temporal lobe epilepsy (TLE), the present study examines the vulnerability of GABAergic subicular interneurons to recurrent seizures and determines its functional implications. In the subiculum of pilocarpine-treated animals, the density of glutamic acid decarboxylase (GAD) mRNA-positive cells was reduced in all layers. Our data indicate a substantial loss of parvalbumin-immunoreactive neurons in the pyramidal cell and molecular layer whereas calretinin-immunoreactive cells were predominantly reduced in the molecular layer. Though the subiculum of pilocarpine-treated rats showed an increased intensity of GAD65 immunoreactivity, the density of GAD65 containing synaptic terminals in the pyramidal cell layer was decreased indicating an increase in the GAD65 intensity of surviving synaptic terminals. We observed a decrease in evoked inhibitory post-synaptic currents that mediate dendritic inhibition as well as a decline in the frequency of miniature inhibitory post-synaptic currents (mIPSCs) that are restricted to the perisomatic region. The decrease in mIPSC frequency (−30%) matched with the reduced number of perisomatic GAD-positive terminals (−28%) suggesting a decrease of pre-synaptic GABAergic input onto pyramidal cells in epileptic animals. Though cell loss in the subiculum has not been considered as a pathogenic factor in human and experimental TLE, our data suggest that the vulnerability of subicular GABAergic interneurons causes an input-specific disturbance of the subicular inhibitory system.

Keywords: subiculum; temporal lobe epilepsy; pilocarpine; GABA; GAD

Abbreviations: ACSF = artificial cerebrospinal fluid; CR-IR = calretinin-immunoreactive; eIPSCs = evoked inhibitory post-synaptic currents; EPSPs = excitatory post-synaptic potential; GAD = glutamic acid decarboxylase; PFA = paraformaldehyde; PV-IR = parvalbumin-immunoreactive; RMP = resting membrane potential; TLE = temporal lobe epilepsy

Received December 10, 2007. Revised April 7, 2008. Accepted April 23, 2008

Introduction

Temporal lobe epilepsy (TLE) is the most common form of adult focal epilepsy. Clinical, pathological and physiological studies have historically emphasized the critical role of the hippocampus in TLE. However, its role in epileptogenesis continues to be a topic of considerable debate. Given that epileptic activity is generated within the mesial temporal lobe with hippocampal areas CA3 and CA1 damaged or even absent, accumulating clinical and experimental evidence suggest that the subiculum and parahippocampal structures play an important role in the maintenance of temporal lobe seizures. Though cell loss in the subiculum is not a significant feature of epilepsy (Fisher *et al.*, 1998; Dawodu and Thom, 2005), previous studies demonstrated that the subiculum but not the hippocampus proper serves as an origin for spontaneous synchronous firing in hippocampal brain slices of patients with TLE (Cohen *et al.*, 2002; Wozny *et al.*, 2003). This spontaneous activity was detected in sclerotic as well as in non-sclerotic tissue and closely resembled the interictal EEG activity recorded from those patients before surgery. The mechanisms that favour spontaneous rhythmic activity by offsetting the frail balance between excitation and inhibition are hitherto not completely understood (Cohen *et al.*, 2003). Recurrent excitatory connectivity of neurons and a high density of pacemaker cells predispose brain regions to generate synchronized activity (Jensen and Yaari, 1997;

Yaari and Beck, 2002). In line with this precondition, the subiculum is characterized by the abundance of burst-spiking pyramidal cells (O'Mara *et al.*, 2001) and by a network connectivity that eases synchronization (Behr and Heinemann, 1996; Harris and Stewart, 2001*a*, *b*).

Impairment of GABA receptor-mediated inhibition may result from the loss of interneurons and has been considered as a critical cause of seizure activity in experimental models of TLE (Magloczky and Freund, 2005). Vulnerability of subpopulations of GABAergic interneurons to seizure-induced damage in experimental models of TLE has been extensively documented for the hilus (Obenaus *et al.*, 1993; Houser and Esclapez, 1996; Buckmaster and Jongen-Relo, 1999) and for CA1 (Houser and Esclapez, 1996; Morin *et al.*, 1998*b*; Andre *et al.*, 2001; Cossart *et al.*, 2001; Dinocourt *et al.*, 2003). Interneurons are heterogeneous with regard to Ca^{2+}-binding proteins and were shown to comprise diverse functional roles in hippocampal networks (Freund and Buzsáki, 1996; Cossart *et al.*, 2001; Mody, 2005). Perisomatic inhibition limits action potential firing, whereas dendritic inhibition primarily controls synaptic integration. Two different interneurons were proposed to play a crucial role in epileptogenesis: parvalbumin- (PV-IR) and calretinin-immunoreactive (CR-IR) interneurons. Predominantly, PV-IR interneurons not only innervate the perisomatic region of principle cells (Kosaka *et al.*, 1987; Braak and Braak, 1991; Seress *et al.*, 1991) but also the dendritic zone (Maccaferri *et al.*, 2000; McBain and Fisahn, 2001). PV-IR interneurons include basket and axo-axonic cells, with an axon innervating the soma and the axon initial segment of pyramidal cells, respectively (Katsumaru *et al.*, 1988). This interneuron subtype limits action potential firing and is responsible for synchronizing principle cell populations during network oscillations (Miles *et al.*, 1996). CR-IR interneurons selectively innervate other interneurons (Gulyas *et al.*, 1996) and are particularly sensitive to epilepsy both in animal models (Magloczky and Freund, 1993; Van Vliet *et al.*, 2004) and in the human epileptic hippocampus (Magloczky *et al.*, 2000). They were proposed to ease synchronous activity by controlling other interneurons terminating on different dendritic and somatic compartments of pyramidal cells (Sloviter, 1987; Gulyas *et al.*, 1996; Morin *et al.*, 1998*a*).

Systemic pilocarpine administration in rats causes an acute convulsive status epilepticus leading to neuronal injury that mimics human hippocampal sclerosis. After a latent period of several weeks following status epilepticus, spontaneous seizures start to occur. Recent studies indicate that in addition to the cholinergic activation of excitatory neurons in specific brain regions, systemic pilocarpine-induced events that increase the permeability of the blood-brain barrier may promote the entry of pilocarpine and serum-derived factors that may contribute to ictogenesis (Marchi *et al.*, 2007; Uva *et al.*, 2008). Using this experimental model of TLE, the present study examines the vulnerability of GABAergic, PV-IR and CR-IR subicular interneurons to excitotoxic damage and determines its functional implications. As the loss of specific GABAergic interneuron subtypes may have distinct pathophysiological consequences, perisomatic and dendritic inhibition is investigated by miniature inhibitory post-synaptic currents (mIPSCs) and evoked inhibitory post-synaptic currents (eIPSCs), respectively. Our data show that in pilocarpine-treated the subiculum is affected by a substantial loss of PV-IR and CR-IR interneurons and of perisomatic GABAergic terminals. We observed a decrease in eIPSCs that mediate dendritic inhibition as well as a decline in the frequency of mIPSCs suggesting a decrease of perisomatic GABAergic input onto pyramidal cells in epileptic animals. Thus, our data demonstrate that the vulnerability of subicular GABAergic interneurons causes an input-specific disturbance of the subicular inhibitory system.

Material and Methods

Pilocarpine-model of epilepsy

The experiments were conducted in accordance with the guidelines of the European Communities Council and were approved by the Regional Berlin Animal Ethics Committee (G 0269/95, G 0328/98). Wistar rats 4- to 5-weeks-old (150–230 g) were injected with the muscarinic agonist pilocarpine (350 mg/kg i.p.). Peripheral cholinergic effects and lethality (9%) were reduced by pre-treatment with methylscopolamine (1 mg/kg s.c.) applied 30 min before pilocarpine administration. Ten to thirty minutes after pilocarpine injection, 77% of the animals developed a generalized convulsive status epilepticus. In order to terminate status epilepticus, diazepam (5–10 mg/kg i.p.) was injected 80 min after onset. The behavioural signs of status epilepticus disappeared about 1 h later. Thereafter, the animals were kept in separate cages on a standard light/dark cycle. A seizure-free interval of about 2 weeks followed the pilocarpine treatment, and after 6–8 weeks the rats (400–600 g) were observed by video recording for 3–10 days. Only animals showing spontaneous seizures were selected for experiments. These animals developed 1.8 ± 0.4 seizures per 24 h ($n = 52$ rats). At the date of preparation the rats were 10- to 21-months-old. Age-matched animals injected with NaCl were used as controls.

Preparation of hippocampal brain slices

Method A

Animals were anaesthetized with isoflurane, perfused through the ascending aorta with paraformaldehyde (PFA, 4% in phosphate buffer, PB) for 15–20 min (20 ml/min) and decapitated. Brains were removed, treated with PFA for further 5 h, stored in 10% saccharose overnight and subsequently stored in 30% saccharose for 1–2 days. After shock freezing in isopentane at −40°C, brains were stored at −70°C. Horizontal sections were cut at 30 µm on a freezing microtome (MICROM GmbH, Germany) and collected as free-floating sections in 0.2 M Tris buffered saline (TBS) containing 0.2% Triton (washing buffer).

Method B

Rats were decapitated under deep isoflurane anaesthesia. The brains were quickly removed, shock frozen by transfer into isopentane at −40°C and stored at −70°C. Horizontal sections

12 µm thick containing the entorhinal cortex, the subiculum and the hippocampus were cut on a cryostat (Leica, Bensheim, Germany), mounted onto Superfrost-Plus slides (Fisher Scientific, Berlin, Germany) and kept at −70°C until use.

Method C

Rats were anaesthetized with diethyl ether and decapitated. Brains were quickly removed and washed with cooled (4°C), aerated (95% O_2, 5% CO_2) artificial cerebrospinal fluid (ACSF) containing in mM: NaCl 129, NaH_2PO_4 1.25, $NaHCO_3$ 21, KCl 3, $CaCl_2$ 1.6, $MgSO_4$ 1.8, glucose 10 at a pH of 7.4. Horizontal slices, 400 µm thick, containing entorhinal cortex, subiculum and hippocampus were cut with a Campden vibroslicer (Loughborough, UK). Subsequently, the slices were stored in an interface chamber continuously perfused with aerated pre-warmed (34°C) ACSF.

NeuN-staining

Horizontal brain sections were prepared from control and pilocarpine-treated rats at an age of 15–19 months by use of method A. Antibodies against NeuN (mouse anti-NeuN 1 : 500, Chemicon, MAB 377) were diluted in washing buffer containing 3% serum. The immunoreaction was visualized using the Vectastain Elite ABC Kit (Vector Laboratories, USA) in combination with biotinylated secondary antibodies (donkey-anti-mouse 1 : 500, Dianova, Germany 711-065-152). NeuN-stained neurons were counted in the molecular, polymorphic and pyramidal cell layer of the subiculum. In the pyramidal cell layer counting of neurons was established in three circular areas ($r = 118.6$ µm) in the proximal, middle and distal region of the subiculum, respectively (Fig. 1A). The pyramidal layer was found to be smaller in pilocarpine-treated compared with control rats, which was caused by the shrinkage of the hippocampus in these animals. Therefore, cell density in pilocarpine-treated rats was corrected by a factor representing the relative shrinkage of the subicular pyramidal cell layer. Computer-assisted cell counting was performed by using ImageJ (Wayne Rasband, NIH, USA).

In situ hybridization

Tissue from control and pilocarpine-treated rats was prepared by use of method B. Cryostat brain sections were fixed in 4% PFA, treated with 0.2 M HCl and acetylated in 0.1 M triethanolamine containing 0.25% acetic anhydride. Digoxigenin-labelled riboprobes (RNA labelling Kit; Boehringer, Mannheim, Germany) for glutamic acid decarboxylase (GAD) 65 and 67 were constructed as described previously (Frahm and Draguhn, 2001). Sense strand hybridizations were processed as a negative control (data not shown). Hybridization was performed for 16 h at 55°C. The digoxigenin-labelled GAD RNA was applied in 200 µl hybridization buffer per slide (InnoGenex, San Ramon, CA, USA). Slides were then washed in a dilutional series of saline-sodium citrate solutions with 0.1% sodium dodecyl sulphate at 55°C. Immunodetection was carried out using a Nucleic Acid Detection Kit (Roche, Mannheim, Germany). Light microscopic analyses were done using an Axioplan 2 microscope coupled with an Axiocam and the Axiovision software (Zeiss, Oberkochen, Germany). For counting of GAD-positive cells, the hippocampus and the subiculum were subdivided into subregions as described in Fig. 1A.

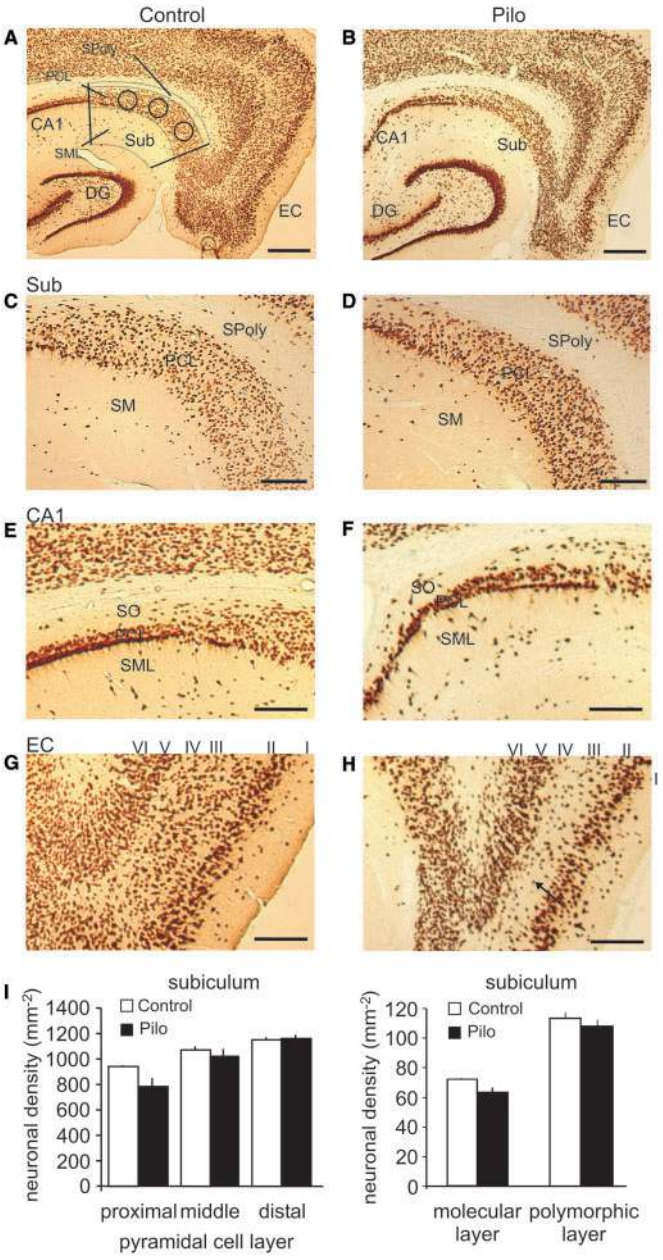

Fig. 1 NeuN stained sections of the hippocampal formation of control (**A, C, E and G**) and pilocarpine-treated (**B, D, F and H**) animals. The subiculum (Sub) consists of a polymorphic layer (SPoly), pyramidal cell layer (PCL) and a molecular layer (SM). In the PCL, cell density is analysed in three circular areas in the proximal, middle and distal part of the PCL (**A**). In the polymorphic and SM, neuronal density is determined by counting NeuN positive cells in the whole layer. (**C**–**H**) High-magnification photomicrographs of the Sub (**C** and **D**), CA1 (**E** and **F**) and the entorhinal cortex (EC) (**G** and **H**) from the same specimens illustrated in **A** and **B**. In pilocarpine-treated animals, a marked reduction in the number of neurons is observed in the PCL of CA1 (**E** and **F**) and in layer III of the entorhinal cortex (**G** and **H**), as indicated by the arrow. This cells loss contrasts with a good preservation of neurons in the Sub of pilocarpine-treated animals (**C** and **D**). (**I**) Bar graphs comparing the mean numbers of NeuN-containing subicular neurons in control (white bars) and pilocarpine-treated (black bars) animals in different layers of the Sub and in the proximal, middle and distal part of the PCL. Scale bars: 0.5 mm in **A–B**, 0.25 mm in **C–H**.

Immunostaining

Horizontal brain slices were prepared by method C, fixed overnight with 4% PFA at 6°C. The slices were cryoprotected by transfer into a 30% sucrose solution at room temperature and cut into 40 µm thick sections by using a freezing microtome (Leitz; Leica Microsystems, Wetzlar, Germany). For Anti-GAD65-staining the sections were cut to 30 µm. Sections were rinsed with PBS, pre-incubated with 3% normal goat serum and then incubated at 6°C for 12 h with the primary monoclonal anti-PV, anti-CR or rabbit anti-GAD65 polyclonal antibody (Chemicon, Germany) diluted 1 : 1000 with 0.3% Triton X-100 in PBS. After washing, the sections were incubated for 12 h at room temperature with Alexa Fluor® 555 or Cy™3 goat anti-rabbit IgG (H + L) conjugate (Zymed, San Francisco, CA), diluted 1 : 1000 in PBS containing 3% normal goat serum. After washing thoroughly with PBS, sections were mounted on gelatin-coated slides, air-dried, placed under a coverslip by use of a non-fluorescent mounting mediums Citifluor AF1 (Agar, Germany) or DePeX (Serva, Heidelberg, Germany) and stored in darkness at 6°C.

Electrophysiology

Horizontal brain slices were prepared by method C. The stimulation electrode was placed nearby the dendritic zone of the recorded pyramidal cell. Recordings were done in the middle portion of the subiculum that receives synaptic input from the middle subfield of CA1 (with respect to the proximo-distal axis of each region) (Amaral *et al.*, 1991).

Intracellular recordings

Intracellular recordings were performed in a liquid-gas interface chamber with sharp microelectrodes (40–100 MΩ) filled with 2.5 M potassium acetate. Recordings were made in bridge mode technique using a SEL 05L or SEL 10 amplifier (npi instruments, Tamm, Germany). Signals were filtered at 3 kHz and sampled at 10 kHz using a TIDA interface card (HEKA, Lambrecht/Pfalz, Germany). IPSCs were evoked with glass-insulated bipolar platinum wire electrodes (tip separation 50–100 µm) by application of 100 µs long pulses at 0.1 Hz.

Patch-clamp recordings

Patch-clamp recordings were performed in a submerged recording chamber in current-clamp whole-cell mode. Visualization of single neurons was established by an Olympus microscope BX51WI equipped with infrared illumination. Patch-clamp electrodes (1.5–5 MΩ) were filled with (in mM): CsCl 130, $MgCl_2$ 2, Na_2ATP 2, NaGTP 0.3, HEPES 10, EGTA 2 at a pH of 7.3 (CsOH). GABAergic chloride currents were isolated by blocking glutamatergic non-NMDA and NMDA receptors with CNQX (30 µM) and DL-APV (60–120 µM), respectively. For recordings of eIPSCs, QX-314 was added to the intracellular solution in order to block fast sodium channels. Recordings of eIPSCs were performed at −35 to −40 mV in order to avoid activation of incompletely blocked fast sodium currents. Under these conditions, the chloride current through GABA-A receptors was directed inwardly. The current could be blocked by the GABA-A receptor antagonist bicuculline methiodide (5 µM). For recordings of mIPSCs, sodium currents were blocked by 0.5 µM TTX added to the ACSF. Recordings of mIPSCs were conducted at −80 mV. In control and pilocarpine-treated animals, mIPSC amplitudes showed a Gaussian distribution. In general, cells were accepted only when the resting membrane potentials (RMP) observed after break through into whole cell mode was more negative than −50 mV. The input resistance R_{in} of a cell was determined with pulses of −10 mV given at −80 mV. Data were collected with an EPC7 patch-clamp amplifier at 3 kHz band width. Recordings and analysis were done using ISO2 software (MFK, Niedernhausen, Germany). All traces were recorded at a sampling rate of 10 kHz (12-bit resolution).

Statistics

Statistical evaluation was performed by applying Levene's test to assess the equality of variance and then by using the appropriate *t*-test (SSPS, SSPS Inc., Chicago, IL, USA). To determine differences in the probability distribution of mIPSCs between control and pilocarpine-treated animals, Kolmogorov-Smirnov test was used. Statistics on cell number/density were conducted by determining the mean number of cells in all slices of one animal, and subsequently comparing the means between animal groups. If not otherwise provided, denoted numbers (n) refer to animals. Data are expressed as means ± SEM. The significance level was set to $P \leqslant 0.05$, if not otherwise stated.

Results

Layer-specific loss of subicular neurons in pilocarpine-treated animals

Neurons of the hippocampal formation were visualized by NeuN to determine the seizure-induced loss of subicular neurons (Fig. 1A–H). Consistent with previous studies (Du *et al.*, 1995; Kobayashi and Buckmaster, 2003; Wozny *et al.*, 2005), slices from pilocarpine-treated rats showed the characteristic degeneration of neurons in the CA1 pyramidal cell layer (Fig. 1E and F) and in layer III of the entorhinal cortex (Fig. 1G and H).

We determined the density of NeuN-stained neuronal somata in the molecular, polymorphic and pyramidal cell layer of the subiculum obtained from control ($n = 5$) and pilocarpine-treated rats ($n = 5$). The pyramidal cell layer was further subdivided into a proximal, middle and distal portion as outlined in the Method section (Fig. 1A). In both, control and pilocarpine-treated animals, neurons in the proximal part of the pyramidal cell layer were only loosely packed. The density increased along the subicular axis showing the highest density in the distal part of the subiculum. We observed no significant difference in the density of NeuN-stained neurons in the pyramidal cell layer between control (1055 ± 9 cells/mm^2) and pilocarpine-treated animals (986 ± 50 cells/mm^2). In the molecular layer, NeuN-stained neurons were inhomogeneously distributed and showed a low density. In control animals, the density of NeuN-stained neurons was 70 ± 2 cells/mm^2. In pilocarpine-treated animals, the density decreased to 62 ± 3 cells/mm^2 ($P < 0.05$). The polymorphic layer showed no significant difference between control (113 ± 4 cells/mm^2) and pilocarpine-treated animals (108 ± 4 cells/mm^2; Fig. 1C, D and I).

Loss of GAD mRNA-containing neurons

Data on seizure-induced degeneration of interneurons depend on various parameters like species, experimental model, seizure history and immunohistochemical methods employed. Vulnerability of subpopulations of GABAergic neurons to seizure-induced damage has been extensively studied in CA1. To achieve comparability between the present and previous studies, we first determined the loss of CA1 interneurons and related it to the loss of subicular interneurons. Using GAD mRNA detection, we assessed the total number of CA1 and subicular interneurons in control and pilocarpine-treated animals. Two isoforms of GABA synthesizing GAD exist: GAD65 and GAD67. They are encoded by two different genes (Erlander *et al.*, 1991) and differ in their intraneuronal localization and functional roles (Erlander and Tobin, 1991; Kaufman *et al.*, 1991; Esclapez *et al.*, 1994). Also the transcription of GAD65 and GAD67 is differentially altered by neuronal activity (Patz *et al.*, 2003). Therefore, *in situ* hybridization was performed with probes recognizing both isoforms in order to label GABA-containing neurons independent of their preference for GAD65 or GAD67 (Kaufman *et al.* 1991; Esclapez *et al.*, 1993; Frahm *et al.*, 2004).

In line with previous studies (Esclapez and Houser, 1999; Houser and Esclapez, 1996; Dinocourt *et al.*, 2003), in CA1 of control animals ($n = 5$) GAD-containing neurons labelled for GAD65 and GAD67 mRNA were distributed in all layers of CA1. The mean density of GAD mRNA positive interneurons was 219 ± 8 cells/mm^2 in the pyramidal cell layer, 149 ± 7 cells/mm^2 in stratum oriens and 67 ± 3 cells/mm^2 in stratum radiatum/stratum lacunosum-moleculare. In the subiculum, the highest density of GAD mRNA-containing cells was found in the pyramidal cell layer (178 ± 7 cells/mm^2), whereas only 103 ± 7 cells/mm^2 and 64 ± 4 cells/mm^2 were labelled in the polymorphic and molecular layer, respectively (Fig. 2A, C and E).

As previously described, in CA1 of pilocarpine-treated animals, we found a selective, layer-specific loss of $23 \pm 9\%$ of GAD-positive cells in stratum oriens ($n = 6$; $P < 0.05$) (Esclapez and Houser, 1999; Andre *et al.*, 2001; Cossart *et al.*, 2001; Dinocourt *et al.*, 2003). In contrast, in the subiculum the density of GAD mRNA-positive cells was reduced in all three layers. In the pyramidal cell and molecular layer, GAD-containing neurons decreased by $28 \pm 8\%$ ($P < 0.01$) and $30 \pm 13\%$ ($P < 0.05$), respectively. The most pronounced loss of subicular interneurons was observed in the polymorphic layer where the number of GAD-positive cells decreased by $46 \pm 14\%$ ($P < 0.01$; Fig. 2B, D and F).

Loss of PV-IR neurons

In control animals ($n = 6$), the majority of PV-positive somata was observed in the pyramidal cell layer (21 ± 6 cells; 96%). Only a small fraction of cells was labelled in the molecular layer (0.6 ± 0.1; 3%) and in the polymorphic layer (0.4 ± 0.1 cells; <2%; Fig. 3A, C and E). In pilocarpine-treated rats ($n = 6$), the most striking loss of PV-IR neurons occurred in the pyramidal cell layer (6 ± 2 cells) and in the molecular layer (0.2 ± 0.1 cells) by 72% ($P < 0.05$) and 66% ($P < 0.05$), respectively. In the polymorphic layer, we observed a less consistent reduction of PV-IR neurons by 48% (0.2 ± 0.1 cells, $P = 0.99$; Fig. 3B, D and E).

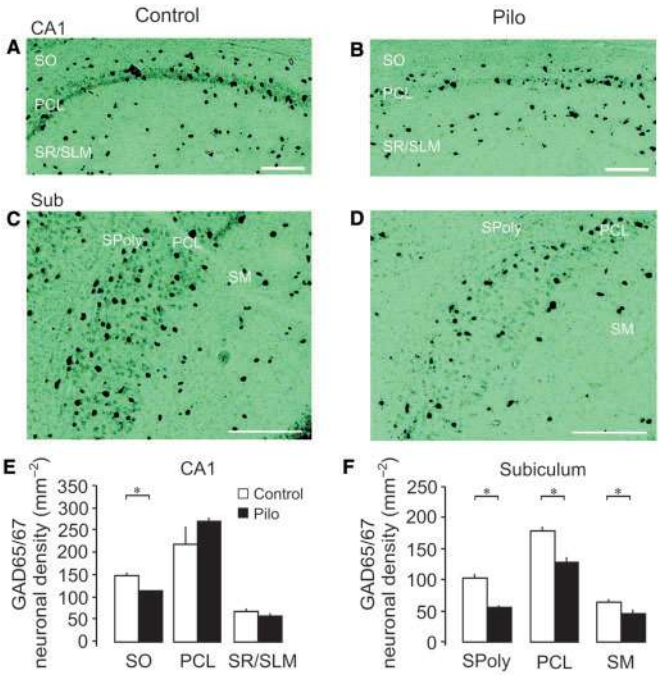

Fig. 2 *In situ* staining of GAD65/67 mRNA in CAI and the Sub of control (**A** and **C**) and pilocarpine-treated (**B** and **D**) animals. In CAI of pilocarpine-treated animals, a selective reduction in the number of neurons is observed in stratum oriens (SO) whereas no significant difference is evident for the PCL and for stratum lacunosum moleculare (SLM) (**A** and **B**). In contrast to the layer-specific loss of GAD mRNA-stained neurons in CAI, in the Sub all three layers (SPoly, PCL, SM) show a significant decrease in the number of GAD mRNA-containing neurons as compared with controls (**C** and **D**). (**E**) Bar graphs comparing the mean numbers of GAD mRNA-containing neurons in control (white bars) and pilocarpine-treated (black bars) animals in different layers of CAI and the Sub Scale bars: 0.25 mm.

Loss of CR-IR neurons

In control animals ($n = 3$), the majority of CR-IR neurons was concentrated in the pyramidal cell layer (10 ± 2 cells; 44%) and in the molecular layer (11 ± 1 cells; 47%;). In the polymorphic layer, only few CR-IR somata were observed (2.1 ± 0.4 cells; 9%; Fig. 4A, C and E). In pilocarpine-treated rats ($n = 3$), a substantial loss of CR-IR was found in the molecular layer (4 ± 1 cells; −63%, $P < 0.01$). In the pyramidal cell layer (6 ± 2 cells; −44%) and polymorphic layer (0.8 ± 0.3 cells; −63%), the loss of CR-IR neurons was less consistent and not significant (Fig. 4B, D and E).

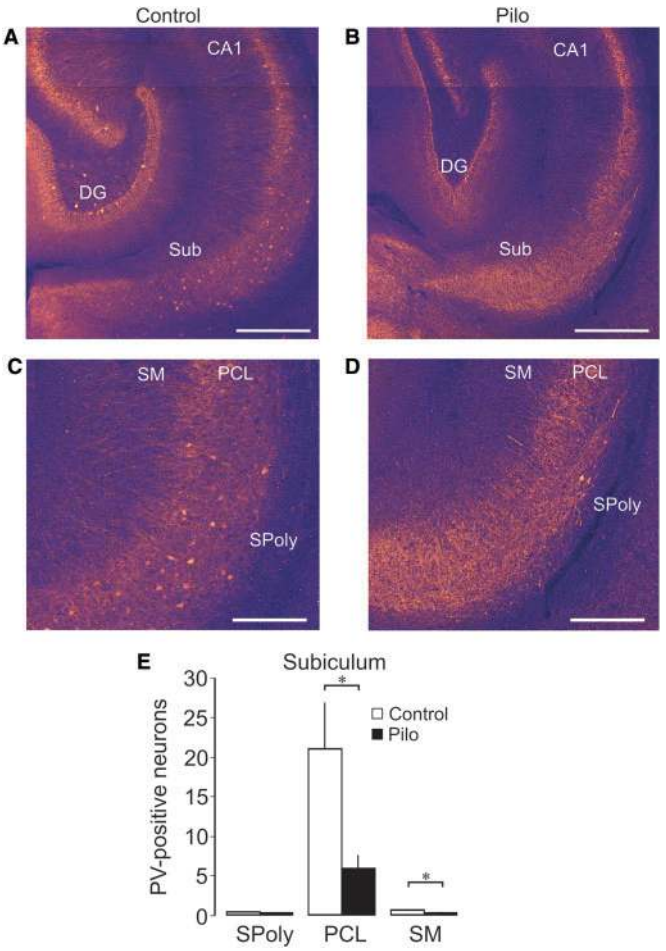

Fig. 3 Immunohistochemical labelling of hippocampal brain slices for parvalbumin (PV) from control (**A**) and pilocarpine-treated (**B**) animals. In control sections, PV-positive somata are mainly concentrated in the pyramidal and granule cell layer of the hippocampal formation. High-magnification photomicrographs from the same specimens illustrated in **A** and **B** show a substantial loss of PV-containing cells in the subicular PCL of pilocarpine-treated (**D**) animals as compared with controls (**C**). Only a minor fraction of PV-containing cells is located in the SPoly and in the SM. (**E**) Bar graphs comparing the mean numbers of PV-containing neurons in control (white bars) and pilocarpine-treated (black bars) animals in different layers of the Sub. Scale bars: 0.5 mm in **A**–**B**, 0.25 mm in **C**–**D**.

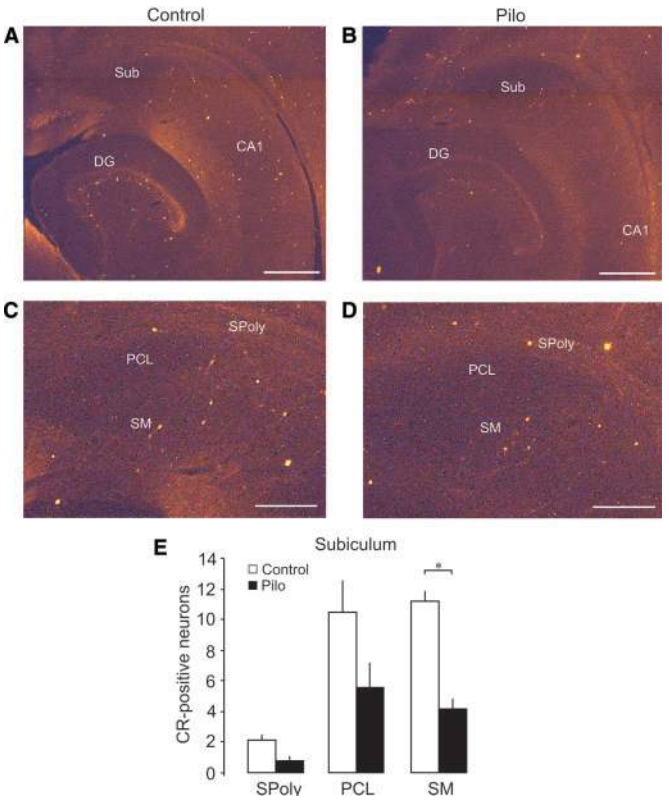

Fig. 4 Immunohistochemical labelling of hippocampal brain slices for CR from control (**A**) and pilocarpine-treated (**B**) animals. In control sections, CR-positive somata are distributed in all layers of the hippocampal formation. High-magnification photomicrographs from the same specimens illustrated in **A** and **B** reveal that in control animals most of the CR-IR neurons are evident in the PCL and SM. In the SPoly only few CR-IR somata are present (**C**). In pilocarpine-treated animals, a significant loss of CR-containing cells occurs in the SM (**D**) as compared with controls. In the pyramidal cell and polymorphic layer, the loss of CR-IR neurons is less consistent. (**E**) Bar graphs comparing the mean numbers of CR-containing neurons in control (white bars) and pilocarpine-treated (black bars) animals in different layers of the Sub. Scale bars: 0.5 mm in **A**–**B**, 0.25 mm in **C**–**D**.

GAD65 immunostaining

Though both isoforms of GAD are present in axon terminals, GAD65 is particularly abundant at these locations (Esclapez and Houser, 1999). Therefore, immunostaining of GAD65 was used to visualize alterations in the pattern of GAD-containing axon terminals in the subiculum. As previously reported (Esclapez and Houser, 1999), in pilocarpine-treated rats, we obtained an increased intensity of GAD65 immunoreactivity in all regions of the hippocampus including the subiculum (control rats: $n = 3$, pilocarpine-treated rats: $n = 3$; Fig. 5A–C). This increase was significantly higher in the pyramidal cell layer (58%, $P < 0.05$) than in the deep and superficial part of the molecular layer of the subiculum (40%, $P < 0.05$ and 35%, $P = 0.06$, respectively; Fig. 5E). The increased intensity of GAD65 immunoreactivity might be due to an increase of the total number or to an enhanced labelling of synaptic terminals. Therefore, we employed confocal microscopy to determine the density of synaptic terminals in control and pilocarpine-treated animals. Like in CA1 (Dinocourt *et al.*, 2003), we found a significant decrease of about 28% in the number of GAD65-containing terminals in the pyramidal cell layer of pilocarpine-treated rats (0.097 ± 0.002 terminals/μm^2 in controls versus 0.07 ± 0.001 terminals/μm^2 in pilocarpine-treated animals, $P < 0.01$; Fig. 5F and G). This result suggests that the increase in GAD immunoreactivity is primarily due to an increase in the GAD load of surviving synaptic terminals but not to their increased number.

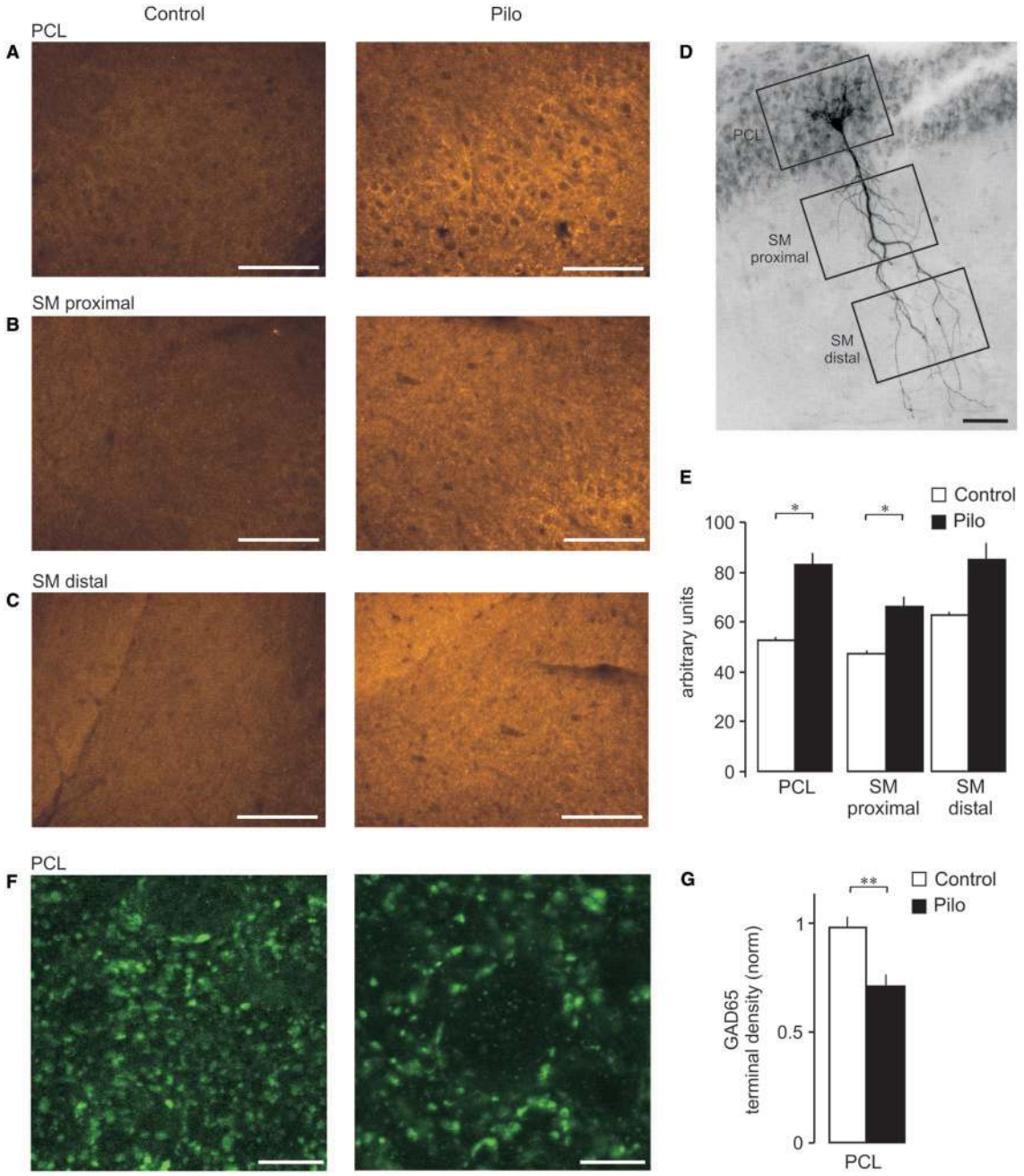

Fig. 5 Immunohistochemical labelling of the Sub for GAD65 from control and pilocarpine-treated animals (**A–C**). In control animals, GAD65 immunoreactivity, which is concentrated in synaptic terminals is predominantly present in the PCL and the dendritic region of the Sub. The Sub of pilocarpine-treated animals shows an increased intensity of GAD65 immunoreactivity that is most pronounced in the PCL (**A**) but also evident in the proximal (**B**) and distal (**C**) region of the SM as compared with control animals. (**D**) Representative pyramidal cell labelled with biocytin showing regions of interest chosen for analysis in **A–C**. (**E**) Bar graphs comparing the mean intensity of GAD65 immunoreactivity in control (white bars) and pilocarpine-treated (black bars) animals in different layers of the Sub. (**F**) Confocal microscopy of GAD65 immunoreactivity in the Sub from control and pilocarpine-treated animals. In pilocarpine-treated animals, a significant decrease in the number of GAD65 containing synaptic terminals is observed in the PCL as compared with control animals. (**G**) Bar graphs comparing the mean density of GAD65-labelled terminals in control (white bars) and pilocarpine-treated (black bars) animals in the PCLs of the Sub. Scale bars: 100 μm in **A–C**, 10 μm in F.

Synaptic properties of subicular pyramidal cells

Like in previous studies (Staff *et al*., 2000; Jung *et al*., 2001; Menendez *et al*., 2003; Knopp *et al*., 2005), subicular pyramidal cells showed a broad variation of discharge behaviour. In both, control and pilocarpine-treated rats, we observed regular-, burst-, strong burst- and high threshold burst-spiking behaviour in response to depolarizing

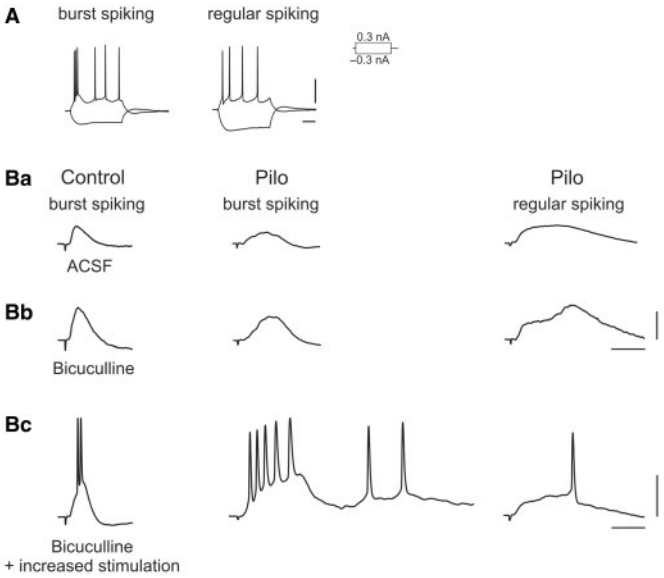

Fig. 6 Evoked EPSPs in subicular pyramidal cells from control and pilocarpine-treated animals. (**A**) Voltage responses of subicular burst-spiking and regular-spiking neurons to depolarizing and hyperpolarizing current pulses. Burst-spiking cell displays single burst discharge followed by single spikes. Regular-spiking cell discharges with a train of single spikes. (**Ba**) EPSPs in control burst-spiking cell and burst- and regular-spiking cell from pilocarpine-treated rat. (**Bb**) In the presence of the $GABA_A$ receptor-antagonist bicuculline, subicular pyramidal cells from control animals show increased EPSP amplitudes. In pilocarpine-treated animals, more than two-thirds of the investigated cells respond with prolonged or polysynaptic EPSPs. (**Bc**) In controls, increasing stimulation intensity results in single action potentials in regular-spiking cells (not shown) or burst firing in burst-spiking cells. In neurons from pilocarpine-treated rats, in 75% of the recordings, increased stimulation intensity causes polysynaptic EPSPs that give rise to single action potentials in regular-spiking cells or long-lasting all-or-none bursts in burst-spiking cells. Scale bars: 10 mV, 25 ms in **Ba** and **Bb**, 25 mV, 25 ms in **Bc**.

current pulses. In control animals, about two-thirds of the cells had been classified as burst-spiking cells (O'Mara *et al.*, 2001). In pilocarpine-treated rats, the majority of cells had been characterized as regular firing cells (Knopp *et al.*, 2005). In control and pilocarpine-treated animals (control animals: $n = 7$ burst-spiking cells, $n = 3$ regular-spiking cells; pilocarpine-treated animals: $n = 9$ burst-spiking cells, $n = 11$ regular-spiking cells; Fig. 6A), stimulation of CA1 efferents elicited excitatory post-synaptic potential (EPSPs) in subicular pyramidal cells (Fig. 6Ba). In the presence of the GABA-A receptor antagonist bicuculline, subicular pyramidal cells from control animals responded with an increased EPSP amplitude. Upon increasing stimulation intensity, they showed either single action potential or burst firing behaviour, depending on the cell type recorded from (burst-spiking cell in Fig. 6Bb and Bc, regular-spiking cell not shown). In neurons from pilocarpine-treated rats, however, in 75% of the recordings we observed prolonged and polysynaptic EPSP responses under GABA-A receptor blockade ($n = 8$ burst-spiking cells, $n = 7$ regular-spiking cells; Fig. 6Bb). After increasing the stimulation intensity, prolonged and polysynaptic EPSPs gave rise to single action potentials in regular-spiking cells and long-lasting all-or-none bursts in burst-spiking cells (Fig. 6Bc).

Evoked IPSCs

eIPSCs primarily cause dendritic inhibition that controls synaptic input and integration in pyramidal cells (Miles *et al.*, 1996). To determine the functional implications of the observed loss of GABAergic interneurons in pilocarpine-treated animals, we analysed eIPSCs in subicular pyramidal cells of control and epileptic animals. Stimulus-response curves were constructed from the normalized eIPSC peak amplitudes plotted versus the stimulation intensity to obtain a measure for the dendritic inhibition in control ($n = 6$) and pilocarpine-treated rats ($n = 11$). The peak eIPSC amplitude increased with stimulation intensity in both preparations. At low stimulation intensities (0.1–0.2 mA), we recorded significantly smaller eIPSC responses in pilocarpine-treated rats compared with controls (Fig. 7A). Using sharp microelectrodes, we analysed stimulus-evoked GABA-A receptor-mediated IPSPs at different membrane potentials in the presence of NMDA, AMPA and GABA-B receptor antagonists. Neither RMP nor reversal potential (U_{rev}) of GABA-A receptor-mediated eIPSPs were significantly different between control (RMP: -62.8 ± 2.2 mV; $U_{rev.}$: -78.7 ± 1.3 mV; $n = 9$) and pilocarpine-treated rats (RMP: -61.3 ± 2.5 mV; $U_{rev.}$: -75.7 ± 4.3 mV; $n = 5$; Fig. 7B). Application of the GABA-A receptor antagonist bicuculline demonstrated that eIPSPs were mediated by GABA-A receptors.

Decreased miniature IPSC activity

Interneurons that selectively innervate the soma of pyramidal cells control the generation of action potentials and the output of pyramidal cells (Miles *et al.*, 1996). Miniature IPSCs result from action-potential-independent release of single GABA-containing vesicles and are restricted to the perisomatic region of pyramidal cells (Otis *et al.*, 1991). In pilocarpine-treated animals, mIPSC frequency was 33% lower than in control animals (14.6 ± 2.0 Hz in controls, $n = 8$, versus 9.9 ± 2.4 Hz in pilocarpine-treated animals, $n = 7$, $P < 0.001$). Miniature IPSC amplitude was decreased by 17% in epileptic animals (35.9 ± 2.5 pA in controls versus 30.1 ± 3.1 pA in pilocarpine-treated animals, $P < 0.001$, Kolmogorov-Smirnov test; Fig. 8). To exclude failures in the detection of decreased mIPSCs in pilocarpine-treated animals that were below the detection threshold and resulted in a reduced frequency, we performed a re-analysis of our data. We adjusted control mIPSC amplitudes to 83% of the original value, re-analysed the frequency of mIPSCs with the same detection threshold and compared the obtained value with the mIPSC frequency of pilocarpine-treated animals. In pilocarpine-treated animals, the frequency was still 33% lower ($P < 0.001$)

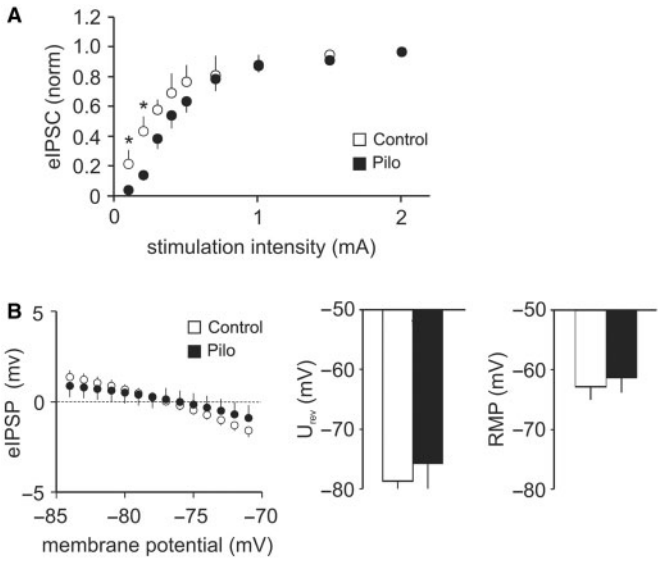

Fig. 7 (**A**) Stimulus-response curve of eIPSCs recorded in subicular pyramidal cells. Peak eIPSC amplitudes increase with stimulation intensity in both preparations. At low stimulation intensities (0.1–0.2 mA), eIPSC responses in pilocarpine-treated rats are significantly smaller compared with controls. (**B**) RMP and reversal potentials (U_{rev}) of eIPSPs recorded with sharp microelectrodes are not different between control and pilocarpine-treated rats. Bicuculline-sensitive $GABA_A$ receptor–mediated responses reverse at hyperpolarized membrane potentials.

than in controls suggesting a pre-synaptic alteration of GABAergic inhibition via a decreased number of perisomatic GABAergic synapses and/or a change in the quantal release probability.

Discussion

Using the pilocarpine model of TLE, this study examines the vulnerability of subicular GABAergic interneurons to recurrent seizures and determines its functional implications. Consistent with previous studies (Du *et al.*, 1995; Kobayashi and Buckmaster, 2003; Wozny *et al.*, 2005), pilocarpine-treated rats showed a characteristic degeneration of NeuN-stained neurons in the CA1 pyramidal cell layer and in layer III of the entorhinal cortex whereas no significant change in the density of neurons was observed in the subicular pyramidal cell layer. While for CA1, we confirmed a selective layer-specific loss of GAD-positive cells in stratum oriens (Houser and Esclapez, 1996; Morin *et al.*, 1998*b*; Esclapez and Houser, 1999; Andre *et al.*, 2001; Cossart *et al.*, 2001; Dinocourt *et al.*, 2003), in the subiculum, the density of GAD mRNA-positive cells was reduced in all three layers. The most striking loss of subicular PV-IR neurons occurred in the pyramidal cell and molecular layer whereas CR-IR cells were predominantly reduced in the molecular layer.

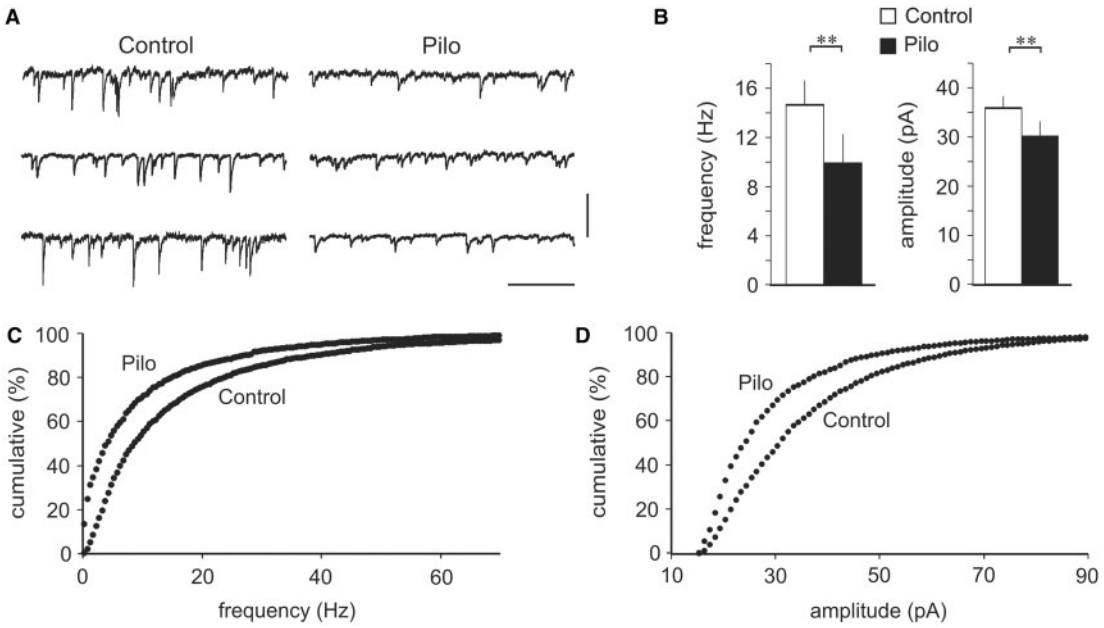

Fig. 8 (**A**): Miniature IPSCs recorded in the presence of TTX, CNQX and APV in subicular pyramidal cells from control and pilocarpine-treated animals. Scale bars: 50 pA, 500 ms. (**B**) Bar graphs comparing the mean frequency and amplitude in control (white bars) and pilocarpine-treated (black bars) animals. In pilocarpine-treated animals, mIPSC frequency is 33% lower than in control animals. mIPSC amplitude is decreased by 17% in epileptic animals. (**C**) Cumulative probability plots of the frequency show a shift to the left in epileptic animals indicating a decreased frequency. (**D**) Cumulative probability plots of the amplitude show a shift to the left in pilocarpine-treated animals indicating decreased mIPSC amplitudes. In control and pilocarpine-treated animals mIPSC amplitudes show a Gaussian distribution.

The vulnerability of PV-IR interneurons in epilepsy is still an open question. In animal models of epilepsy and in the human epileptic hippocampus, survival (Best *et al.*, 1993; Maglóczky and Freund, 1995; Buckmaster and Dudek, 1997; Zhu *et al.*, 1997) as well as loss of PV-IR interneurons (Sloviter *et al.*, 1991; Arellano *et al.*, 2004) has been observed. Studies in animal models of ischemia and epilepsy as well as human studies have provided evidence for a transient decrease of immunoreactivity from the soma and dendrites of interneurons (Johansen *et al.*, 1990; Tortosa and Ferrer 1993; Bazzett *et al.*, 1994; Maglóczky and Freund, 1995). Studying the distribution of PV-IR interneurons in CA1 as well as the synaptic input of CA1 pyramidal cell somata and axon initial segments of human control subjects and patients with TLE, Wittner *et al.* suggested that PV-IR interneurons may survive as long as their targets are present (Wittner *et al.*, 2005). Though the subiculum of pilocarpine-treated rats showed an overall increased intensity of GAD65 immunoreactivity, probably due to an enhanced metabolic activity, the total number of GAD65 containing synaptic terminals in the pyramidal cell layer was decreased indicating an increase in the GAD65 intensity of surviving synaptic terminals. In different epilepsy models as well as in human TLE an increase of GAD mRNA has been described (Feldblum *et al.*, 1990; Najlerahim *et al.*, 1992; Neder *et al.*, 2002). In particular, CA1 of pilocarpine-treated animals showed an increased intensity of GAD65 immunoreactivity (Esclapez and Houser, 1999) that was associated with a decrease of GABAergic synaptic terminals. The reduction in the number of boutons in the CA1 pyramidal cell layer has been attributed to the selective loss of PV-IR axo-axonic cells (Dinocourt *et al.*, 2003). Though in the present study, a transient seizure-induced decrease of subicular PV-IR cannot be excluded, the reduced number of GAD65 containing perisomatic terminals favours a loss of PV-IR interneurons.

The loss of GABAergic interneurons may shift the balance of excitation and inhibition towards excitation (Ben-Ari and Represa, 1990) thereby increasing the probability to generate spontaneous recurrent discharges as observed in the subicular network of pilocarpine-treated rats (Knopp *et al.*, 2005) as well as in the epileptic human subiculum (Cohen *et al.*, 2002; Wozny *et al.*, 2003). The subiculum of pilocarpine-treated rats showed an enhanced network excitability characterized by polysynaptic responses as previously described (Knopp *et al.*, 2005; de Guzman *et al.*, 2006). The remaining $GABA_A$ receptor-mediated synaptic inhibition seems to be of particular importance for controlling the excitatory network in pilocarpine-treated animals. Once eliminated, as accomplished in the present study by pharmacological GABA-A receptor blockade, the strong potential of the recurrent excitatory subicular network to produce long-lasting EPSP responses and epileptiform discharges is unleashed. Taking into account that burst-spiking pyramidal cells are believed to be important for the generation of synchronized activity (Jensen and Yaari, 1997; Yaari and Beck, 2002), these observations are in line with studies that suggest an inhibitory control of subicular burst-spiking neurons by local interneurons (Menendez, 2003).

To determine the functional implications of the substantial loss of perisomatic PV-containing cells and of GABAergic synaptic terminals in more detail, we examined perisomatic inhibition mediated by mIPSCs. We detected a decrease of mIPSC frequency by 30% in pilocarpine-treated animals. Similar results were previously obtained in CA1 (Hirsch *et al.*, 1999). However, in CA1 the decrease of mIPSC frequency was 2-fold as compared with our study. Interestingly, the decrease in mIPSC frequency (−30%) matched with the reduced number of perisomatic GAD-positive terminals (−28%) in the subicular pyramidal cell layer suggesting a decrease of pre-synaptic GABAergic input onto pyramidal cells in epileptic animals. As perisomatic inhibition supplied by mIPSCs may derive from axo-axonic cells (Hirsch *et al.*, 1999), the loss of PV-containing cells may cause the decrease of mIPSC frequency.

It is difficult to determine the pathophysiological implication of the loss of CR-containing cells. As CR-IR hippocampal interneurons selectively innervate and control other interneurons that terminate on different dendritic and somatic compartments of principal cells (Sloviter, 1987; Gulyas *et al.*, 1996; Morin *et al.*, 1998*a*) their degeneration might result in disinhibition of dendritic inhibitory cells. As the functional role of subicular CR-containing cells is not clear, attempts to discuss the pathophysiological implications of the reduced number of these cells in epileptic rats are highly speculative. In addition, due to the differences between the rat (Gulyas *et al.*, 1996) and human hippocampus (Nitsch and Ohm, 1995; Urban *et al.*, 2002) in the heterogeneity and connectivity of CR-IR cells, findings from animal models can hardly be translated into humans. In the present study, we observed no substantial decrease in the strength of evoked inhibition primarily mediated by inhibitory dendritic input to principal cells (Miles *et al.*, 1996). This result suggests that surviving interneurons remain functional, as indicated by the enhanced intensity of GAD65 immunoreactivity and compensate to some extent for the impaired dendritic inhibition.

Previous studies in human (Cohen *et al.*, 2002; Palma *et al.*, 2005) and experimental (de Guzman *et al.*, 2006) epileptic tissue reported that the reversal potential of GABA-A receptor-mediated responses in subicular pyramidal cells is more positive than under control conditions. This effect has been attributed to an accumulation of intracellular chloride ions resulting from a reduced expression of the neuron-specific potassium-chloride co-transporter 2 (KCC2) (Cohen *et al.*, 2002; Rivera *et al.*, 2004; Palma *et al.*, 2005; de Guzman *et al.*, 2006) and a increased expression of the sodium-potassium-chloride co-transporter NKCC1 (Palma *et al.*, 2005). Such a decrease in reversal potential may

account for depolarizing GABAergic events and the induction of spontaneous rhythmic activity in the subicular network. In contrast to these studies, we found no evidence for a decrease in the reversal potential of eIPSPs in tissue obtained from pilocarpine-treated animals. Bicuculline-sensitive GABA-A receptor-mediated responses always reversed at hyperpolarized membrane potentials. So far, we have no conclusive explanation for this discrepancy. There is some evidence that in human epileptic tissue inhibitory interneurons might function as pacemaker cells driving spontaneous activity in the subicular network via depolarizing GABAergic signalling (Cohen *et al.*, 2002). However, only in a subgroup of 22% of pacemaker cells, Cohen *et al.* observed such depolarizing events. Though spontaneous rhythmic activity has also been observed by us and others in the pilocarpine-model of TLE (Knopp *et al.*, 2005; de Guzman *et al.*, 2006), in our hands, this type of activity has not been found consistently. Given the hypothesis that depolarizing GABAergic events may contribute to the generation of spontaneous activity, the absence of this network activity and/or a low fraction of pacemaker cells that show depolarizing events might be a reason for the lack of excitatory GABA-A receptor-mediated responses in the present study.

Subicular pyramidal cells in epileptic tissue seem to be restrained by a strong local GABAergic network (Menendez, 2003). The substantial loss of GABAergic interneurons observed by us and others (Van Vliet *et al.*, 2004; de Guzman *et al.*, 2006) in epileptic tissue involves a decrease of dendritic and perisomatic inhibition. Though cell loss in the subiculum has not been considered as a pathogenic factor in human (Fisher *et al.*, 1998; Wozny *et al.*, 2003; Dawodu and Thom, 2005) and experimental TLE (Knopp *et al.*, 2005), our data suggest that the vulnerability of GABAergic interneurons gives rise to an input-specific impairment of inhibition.

Acknowledgements

This work was supported by the German Research foundation (DFG) grant SFB-TR3 to J. Behr.

References

Amaral DG, Dolorfo C, Alvarez-Royo P. Organization of CA1 projections to the subiculum: a PHA-L analysis in the rat. Hippocampus 1991; 1: 415–36.

Andre V, Marescaux C, Nehlig A, Fritschy JM. Alterations of hippocampal GAbaergic system contribute to development of spontaneous recurrent seizures in the rat lithium-pilocarpine model of temporal lobe epilepsy. Hippocampus 2001; 11: 452–68.

Arellano JI, Munoz A, Ballesteros-Yanez I, Sola RG, DeFelipe J. Histopathology and reorganization of chandelier cells in the human epileptic sclerotic hippocampus. Brain 2004; 127: 45–64.

Bazzett TJ, Becker JB, Falik RC, Albin RL. Chronic intrastriatal quinolinic acid produces reversible changes in perikaryal calbindin and parvalbumin immunoreactivity. Neuroscience 1994; 60: 837–41.

Behr J, Heinemann U. Low Mg^{2+} induced epilptiform activity in the subiculum before and after disconnection from rat hippocampal and entorhinal cortex slices. Neurosci Lett 1996; 205: 25–8.

Ben-Ari Y, Represa A. Brief seizure episodes induce long-term potentiation and mossy fibre sprouting in the hippocampus. Trends Neurosci 1990; 13: 312–8.

Best N, Mitchell J, Baimbridge KG, Wheal HV. Changes in parvalbumin-immunoreactive neurons in the rat hippocampus following a kainic acid lesion. Neurosci Lett 1993; 155: 1–6.

Braak H, Braak E. Neuropathological stageing of Alzheimer-related changes. Acta Neuropathol (Berl) 1991; 82: 239–59.

Buckmaster PS, Dudek FE. Neuron loss, granule cell axon reorganization, and functional changes in the dentate gyrus of epileptic kainate-treated rats. J Comp Neurol 1997; 385: 385–404.

Buckmaster PS, Jongen-Relo AL. Highly specific neuron loss preserves lateral inhibitory circuits in the dentate gyrus of kainate-induced epileptic rats. J Neurosci 1999; 19: 9519–29.

Cohen I, Navarro V, Clemenceau S, Baulac M, Miles R. On the origin of interictal activity in human temporal lobe epilepsy in vitro. Science 2002; 298: 1418–21.

Cohen I, Navarro V, Le Duigou C, Miles R. Mesial temporal lobe epilepsy: a pathological replay of developmental mechanisms? Biol Cell 2003; 95: 329–33.

Cossart R, Dinocourt C, Hirsch JC, et al. Dendritic but not somatic GABAergic inhibition is decreased in experimental epilepsy. Nat Neurosci 2001; 4: 52–62.

Dawodu S, Thom M. Quantitative neuropathology of the entorhinal cortex region in patients with hippocampal sclerosis and temporal lobe epilepsy. Epilepsia 2005; 46: 23–30.

de Guzman P, Inaba Y, Biagini G, Baldelli E, Mollinari C, Merlo D, et al. Subiculum network excitability is increased in a rodent model of temporal lobe epilepsy. Hippocampus 2006; 16: 843–60.

Dinocourt C, Petanjek Z, Freund TF, Ben Ari Y, Esclapez M. Loss of interneurons innervating pyramidal cell dendrites and axon initial segments in the CA1 region of the hippocampus following pilocarpine-induced seizures. J Comp Neurol 2003; 459: 407–25.

Du F, Eid T, Lothman EW, Köhler C, Schwarcz R. Preferential neuronal loss in layer III of the medial entorhinal cortex in rat models of temporal lobe epilepsy. J Neurosci 1995; 15: 6301–13.

Erlander MG, Tillakaratne NJ, Feldblum S, Patel N, Tobin AJ. Two genes encode distinct glutamate decarboxylases. Neuron 1991; 7: 91–100.

Erlander MG, Tobin AJ. The structural and functional heterogeneity of glutamic acid decarboxylase: a review. Neurochem Res 1991; 16: 215–26.

Esclapez M, Houser CR. Up-regulation of GAD65 and GAD67 in remaining hippocampal GABA neurons in a model of temporal lobe epilepsy. J Comp Neurol 1999; 412: 488–505.

Esclapez M, Tillakaratne NJ, Kaufman DL, Tobin AJ, Houser CR. Comparative localization of two forms of glutamic acid decarboxylase and their mRNAs in rat brain supports the concept of functional differences between the forms. J Neurosci 1994; 14: 1834–55.

Esclapez M, Tillakaratne NJK, Tobin AJ, Houser CR. Comparative localization of mRNAs encoding two forms of glutamic acid decarboxylase with nonradioactive in situ hybridization methods. J Comp Neurol 1993; 331: 339–62.

Feldblum S, Ackermann RF, Tobin AJ. Long-term increase of glutamate decarboxylase mRNA in a rat model of temporal lobe epilepsy. Neuron 1990; 5: 361–71.

Fisher PD, Sperber EF, Moshe SL. Hippocampal sclerosis revisited. Brain Dev 1998; 20: 563–73.

Frahm C, Draguhn A. GAD and GABA transporter (GAT-1) mRNA expression in the developing rat hippocampus. Brain Res Dev Brain Res 2001; 132: 1–13.

Frahm C, Haupt C, Witte OW. GABA neurons survive focal ischemic injury. Neuroscience 2004; 127: 341–6.

Freund TF, Buzsáki G. Interneurons of the hippocampus. Hippocampus 1996; 6: 347–470.

Gulyas AI, Hajos N, Freund TF. Interneurons containing calretinin are specialized to control other interneurons in the rat hippocampus. J Neurosci 1996; 16: 3397–411.

Harris E, Stewart M. Intrinsic connectivity of the rat subiculum: II. Properties of synchronous spontaneous activity and a demonstration of multiple generator regions. J Comp Neurol 2001a; 435: 506–18.

Harris E, Stewart M. Propagation of synchronous epileptiform events from subiculum backward into area CA1 of rat brain slices. Brain Res 2001b; 895: 41–9.

Hirsch JC, Agassandian C, Merchan-Perez A, Ben Ari Y, DeFelipe J, Esclapez M, et al. Deficit of quantal release of GABA in experimental models of temporal lobe epilepsy. Nat Neurosci 1999; 2: 499–500.

Houser CR, Esclapez M. Vulnerability and plasticity of the GABA system in the pilocarpine model of spontaneous recurrent seizures. Epilepsy Res 1996; 26: 207–18.

Jensen MS, Yaari Y. Role of intrinsic burst firing, potassium accumulation, and electrical coupling in the elevated potassium model of hippocampal epilepsy. J Neurophysiol 1997; 77: 1224–33.

Johansen FF, Tonder N, Zimmer J, Baimbridge KG, Diemer NH. Short-term changes of parvalbumin and calbindin immunoreactivity in the rat hippocampus following cerebral ischemia. Neurosci Lett 1990; 120: 171–4.

Jung HY, Staff NP, Spruston N. Action potential bursting in subicular pyramidal neurons is driven by a calcium tail current. J Neurosci 2001; 21: 3312–21.

Katsumaru H, Kosaka T, Heizmann CW, Hama K. Immunocytochemical study of GABAergic neurons containing the calcium-binding protein parvalbumin in the rat hippocampus. Exp Brain Res 1988; 72: 347–62.

Kaufman DL, Houser CR, Tobin AJ. Two forms of the gamma-aminobutyric acid synthetic enzyme glutamate decarboxylase have distinct intraneuronal distributions and cofactor interactions. J Neurochem 1991; 56: 720–3.

Knopp A, Kivi A, Wozny C, Heinemann U, Behr J. Cellular and network properties of the subiculum in the pilocarpine model of temporal lobe epilepsy. J Comp Neurol 2005; 483: 476–88.

Kobayashi M, Buckmaster PS. Reduced inhibition of dentate granule cells in a model of temporal lobe epilepsy. J Neurosci 2003; 23: 2440–52.

Kosaka T, Katsumaru H, Hama K, Wu J-Y, Heizmann CW. GABAergic neurons containing the Ca^{2+}-binding protein parvalbumin in the rat hippocampus and dentate gyrus. Brain Res 1987; 419: 119–30.

Maccaferri G, Roberts JD, Szucs P, Cottingham CA, Somogyi P. Cell surface domain specific postsynaptic currents evoked by identified GABAergic neurones in rat hippocampus in vitro. J Physiol 2000; 524 (Pt 1): 91–116.

Magloczky Z, Freund TF. Selective neuronal death in the contralateral hippocampus following unilateral kainate injections into the CA3 subfield. Neuroscience 1993; 56: 317–35.

Maglóczky Z, Freund TF. Delayed cell death in the contralateral hippocampus following kainate injection into the CA3 subfield. Neuroscience 1995; 66: 847–60.

Magloczky Z, Freund TF. Impaired and repaired inhibitory circuits in the epileptic human hippocampus. Trends Neurosci 2005; 28: 334–40.

Magloczky Z, Wittner L, Borhegyi Z, Halasz P, Vajda J, Czirjak S, et al. Changes in the distribution and connectivity of interneurons in the epileptic human dentate gyrus. Neuroscience 2000; 96: 7–25.

Marchi N, Oby E, Batra A, Uva L, de Curtis M, Hernandez N, et al. In vivo and in vitro effects of pilocarpine: relevance to ictogenesis. Epilepsia 2007; 48: 1934–46.

McBain CJ, Fisahn A. Interneurons unbound. Nat Rev Neurosci 2001; 2: 11–23.

Menendez dlP. Control of bursting by local inhibition in the rat subiculum in vitro. J Physiol 2003; 549: 219–30.

Menendez dlP, Suarez F, Pozo MA. Electrophysiological and morphological diversity of neurons from the rat subicular complex in vitro. Hippocampus 2003; 13: 728–44.

Miles R, Tóth K, Gulyás AI, Hájos N, Freund TF. Differences between somatic and dendritic inhibition in the hippocampus. Neuron 1996; 16: 815–23.

Mody I. Aspects of the homeostaic plasticity of GABAA receptor-mediated inhibition. J Physiol 2005; 562: 37–46.

Morin F, Beaulieu C, Lacaille JC. Cell-specific alterations in synaptic properties of hippocampal CA1 interneurons after kainate treatment. J Neurophysiol 1998a; 80: 2836–47.

Morin F, Beaulieu C, Lacaille JC. Selective loss of GABA neurons in area CA1 of the rat hippocampus after intraventricular kainate. Epilepsy Res 1998b; 32: 363–9.

Najlerahim A, Williams SF, Pearson RCA, Jefferys JGR. Increased expression of GAD mRNA during the chronic epileptic syndrome due to intrahippocampal tetanus toxin. Exp Brain Res 1992; 90: 332–42.

Neder L, Valente V, Carlotti CG Jr, Leite JP, Assirati JA, Paco-Larson ML, et al. Glutamate NMDA receptor subunit R1 and GAD mRNA expression in human temporal lobe epilepsy. Cell Mol Neurobiol 2002; 22: 689–98.

Nitsch R, Ohm TG. Calretinin immunoreactive structures in the human hippocampal formation. J Comp Neurol 1995; 360: 475–87.

O'Mara SM, Commins S, Anderson M, Gigg J. The subiculum: a review of form, physiology and function. Prog Neurobiol 2001; 64: 129–55.

Obenaus A, Esclapez M, Houser CR. Loss of glutamate decarboxylase mRNA-containing neurons in the rat dentate gyrus following pilocarpine-induced seizures. J Neurosci 1993; 13: 4470–85.

Otis TS, Staley KJ, Mody I. Perpetual inhibitory activity in mammalian brain slices generated by spontaneous GABA release. Brain Res 1991; 545: 142–50.

Palma E, Spinelli G, Torchia G, Martinez-Torres A, Ragozzino D, Miledi R, et al. Abnormal GABAA receptors from the human epileptic hippocampal subiculum microtransplanted to Xenopus oocytes. Proc Natl Acad Sci USA 2005; 102: 2514–8.

Patz S, Wirth MJ, Gorba T, Klostermann O, Wahle P. Neuronal activity and neurotrophic factors regulate GAD-65/67 mRNA and protein expression in organotypic cultures of rat visual cortex. Eur J Neurosci 2003; 18: 1–12.

Rivera C, Voipio J, Thomas-Crusells J, Li H, Emri Z, Sipila S, et al. Mechanism of activity-dependent downregulation of the neuron-specific K-Cl cotransporter KCC2. J Neurosci 2004; 24: 4683–91.

Seress L, Gulyas AI, Freund TF. Parvalbumin- and Calbindin D_{28k}-immunoreactive neurons in the hippocampal formation of the Macaque monkey. J Comp Neurol 1991; 313: 162–77.

Sloviter RS. Decreased hippocampal inhibition and a selective loss of interneurons in experimental epilepsy. Science 1987; 235: 73–6.

Sloviter RS, Sollas AL, Barbaro NM, Laxer KD. Calcium-binding protein (calbindin-D28K) and parvalbumin immunocytochemistry in the normal and epileptic human hippocampus. J Comp Neurol 1991; 308: 381–96.

Staff NP, Jung HY, Thiagarajan T, Yao M, Spruston N. Resting and active properties of pyramidal neurons in subiculum and CA1 of rat hippocampus. J Neurophysiol 2000; 84: 2398–408.

Tortosa A, Ferrer I. Parvalbumin immunoreactivity in the hippocampus of the gerbil after transient forebrain ischaemia: a qualitative and quantitative sequential study. Neuroscience 1993; 55: 33–43.

Urban Z, Magloczky Z, Freund TF. Calretinin-containing interneurons innervate both principal cells and interneurons in the CA1 region of the human hippocampus. Acta Biol Hung 2002; 53: 205–20.

Uva L, Librizzi L, Marchi N, Noe F, Bongiovanni R, Vezzani A, et al. Acute induction of epileptiform discharges by pilocarpine in the in vitro isolated guinea-pig brain requires enhancement of blood-brain barrier permeability. Neuroscience 2008; 151: 303–12.

Van Vliet EA, Aronica E, Tolner EA, Lopes da Silva FH, Gorter JA. Progression of temporal lobe epilepsy in the rat is associated with immunocytochemical changes in inhibitory interneurons in specific regions of the hippocampal formation. Exp Neurol 2004; 187: 367–79.

Wittner L, Eross L, Czirjak S, Halasz P, Freund TF, Magloczky Z. Surviving CA1 pyramidal cells receive intact perisomatic inhibitory input in the human epileptic hippocampus. Brain 2005; 128: 138–52.

Wozny C, Gabriel S, Jandova K, Schulze K, Heinemann U, Behr J. Entorhinal cortex entrains epileptiform activity in CA1 in pilocarpine-treated rats. Neurobiol Dis 2005; 19: 451–60.

Wozny C, Kivi A, Lehmann TN, Dehnicke C, Heinemann U, Behr J. Comment on 'On the origin of interictal activity in human temporal lobe epilepsy in vitro'. Science 2003; 301: 463.

Yaari Y, Beck H. 'Epileptic neurons' in temporal lobe epilepsy. Brain Pathol 2002; 12: 234–9.

Zhu ZQ, Armstrong DL, Hamilton WJ, Grossman RG. Disproportionate loss of CA_4 parvalbumin-immunoreactive interneurons in patients with Ammon's horn sclerosis. J Neuropathol Exp Neurol 1997; 56: 988–98.